ZU-TH XX/22

Mixed QCD–EW corrections to neutral current Drell-Yan

Abstract

June 2022

1 Introduction

2 Phenomenological results

2.1 Resonant production

We first study the impact of the mixed corrections on the bulk of the Drell-Yan cross section around the Z peak. We consider the production of a pair of massive muons in proton-proton collisions at $\sqrt{s} = 13.6\,\text{TeV}$ considering a fiducial volume inspired by ATLAS and CMS precision measurements of the Z properties [], namely

$$p_{T,\mu} > 25\,\text{GeV}, \quad |y_\mu| < 2.5, \quad 66\,\text{GeV} < m_{\mu\mu} < 116\,\text{GeV}\,. \tag{1}$$

We adopt the complex mass scheme [] for the treatment of the unstable weak resonance and the G_μ input scheme with the following EW on shell parameters: $M_{Z,\text{OS}} = 91.1876\,\text{GeV}$, $\Gamma_{Z,\text{OS}} = 2.4952\,\text{GeV}$, $\Gamma_{W,\text{OS}} = 80.385\,\text{GeV}$ and $\Gamma_{W,\text{OS}} = 2.085\,\text{GeV}$. The central renormalisation and factorisation scales are set equal to the mass of the Z boson, $\mu_\text{R} = \mu_\text{F} = M_Z$. In the following results, the theoretical uncentainties are estimated by the customary 7-point scale variation, i.e. by varying the μ_R and μ_F scales by a factor of two around their central values with the constraint $1/2 < \mu_\text{R}/\mu_\text{F} < 2$.

In Table 1, we show our predictions for the fiducial cross section with an increasing radiative content. Focusing first on only QCD effects, we observe that the NLO QCD correction increases the fiducial cross section by about 5% with respect to the LO and leads to a reduction of the theoretical uncertainties to about 4%. The NNLO QCD K-factor is close to unity while the associated error band gets shrinked at the 1% percent level or better. LB

(Add comment on results at N3LO; theoretical uncertainties are underestimated at NNLO)

Moving to the EW corrections, we observe a larger K-factor than what expected by a naive coupling counting. Indeed, the NLO EW correction is similar in size to the NLO QCD one and, being negative, largely compensates the latter. The mixed QCD-EW correction is smaller by an order of magnitude, but larger than the NNLO QCD one. LB

(Shall we comment on the fact that the inclusion of mixed corrections does not help (the correction goes in the right direction, but the magnitude is too small) to reconcile the NNLOvsN3LO non-overlapping issue. I think that of course, assuming a pure QCD model (which is is legitimate), one cannot advocate EW effects as a solution.)

The choice of the EW input scheme represents another relevant source of theoretical uncertainty. We repeated the calculation using the α_0-scheme. The results are shown in Table 2 *(Mixed results still missing because of the lack of the corresponding two-loop grid. Add comments.)* LB

We now turn to differential distributions. In the left plot of Figure 1, we show results for the rapidity distribution of the di-muon system. The shape of the NLO-EW correction is rather flat and in line with the fiducial K-factor, while the mixed QCD-EW one displays a less trivial

G_μ-scheme	σ [pb]	$\sigma^{(i,j)}$ [pb]	$\sigma^{(i,j)}/\sigma_{\rm LO}$
LO	$763.40(2)^{+12.7\%}_{-13.6\%}$	–	–
NLO QCD	$802.26(6)^{+2.7}_{-4.2\%}$	38.86(6)	5.1%
NNLO QCD	$802.5(7)^{+0.4}_{-0.8\%}$	0.2(7)	0.0%
NLO EW	$730.76(2)^{+12.7}_{-13.6\%}$	−32.65(3)	−4.3%
NNLO QCD+EW	$769.8(7)^{+0.5}_{-0.6\%}$	–	–
NNLO QCD+EW+MIX$_{\rm fact}$	$768.2(7)^{+0.3}_{-0.7\%}$	−2.0(1)	−0.2%
NNLO QCD+EW+MIX	$772.4(8)^{+0.3}_{-0.7\%}$	2.6(2)	0.3%

Table 1: Predictions using

α_0-scheme	σ [pb]	$\sigma^{(i,j)}$ [pb]	$\sigma^{(i,j)}/\sigma_{\rm LO}$
LO	$712.16(1)^{+12.7\%}_{-13.6\%}$	–	–
NLO QCD	$748.34(2)^{+2.7}_{-4.2\%}$	36.18(3)	5.1%
NNLO QCD	$748.5(7)^{+0.4}_{-0.8\%}$	0.2(7)	0.0%
NLO EW	$735.18(1)^{+12.7}_{-13.6\%}$	23.02(2)	3.2%
NNLO QCD+EW	$771.5(7)^{+0.8}_{-1.2\%}$	–	–
NNLO QCDxEWqq	$772.7(7)^{+0.4}_{-0.8\%}$	1.0(1)	0.2%
NNLO QCD+EW+MIX	$772.5(7)^{+1.7}_{-2.1\%}$	1.0(2)	0.1%

Table 2: As in Table 1 for the computation performed in the α_0-scheme.

pattern. The latter gives a relatively large 1% positive effect in the central rapidity region and becomes negative towards the tail with a turning point around $|y_{\mu\mu}| = 1.4$. Therefore, the smallness of the mixed correction at the level of the integrated fiducial cross section is a consequence of averaging over positive and negative values. On the other hand, there are varius regions in which the mixed QCD-EW correction is enhanced at the 1% level. We notice that a similar behavior, with a turning point occurring around the same region, is already present for the NLO-QCD correction, as reported in the bottom panel, where the NLO-EW and NLO-QCD differential K-factors are displayed. We observe that also the prediction obtained using the factorised ansatz displays a similar pattern. Nontheless, it fails to reproduce the enhancement of the correction in the central region, which seems a genuine effect of the exact result.

In the right plot of Figure 1, we consider the invariant mass distribution of the di-muon system. QCD radiative corrections are generally mild for this observable, while the emission of QED radiation off the final-state lepton pair has a significant impact if the invariant mass is reconstructed from bare leptons, as we do here. The inclusion of the NLO-EW correction leads indeed to a shift of the events with the formation of the characteristic radiative tail in the region at the left of the peak. Focusing on the impact of the mixed QCD-EW correction in the middle plot, we observe sizeable effects and a non-trivial shape. The correction is vanishing around the peak, where it reaches the maximum slope, while is rather flat, positive and around 4% in the region before the peak and rather flat, negative and around −2% in the region after. We observe that the prediction obtained with the factorised ansatz works well in the latter region, while fails to describe the exact result towards smaller invariant masses. This signals

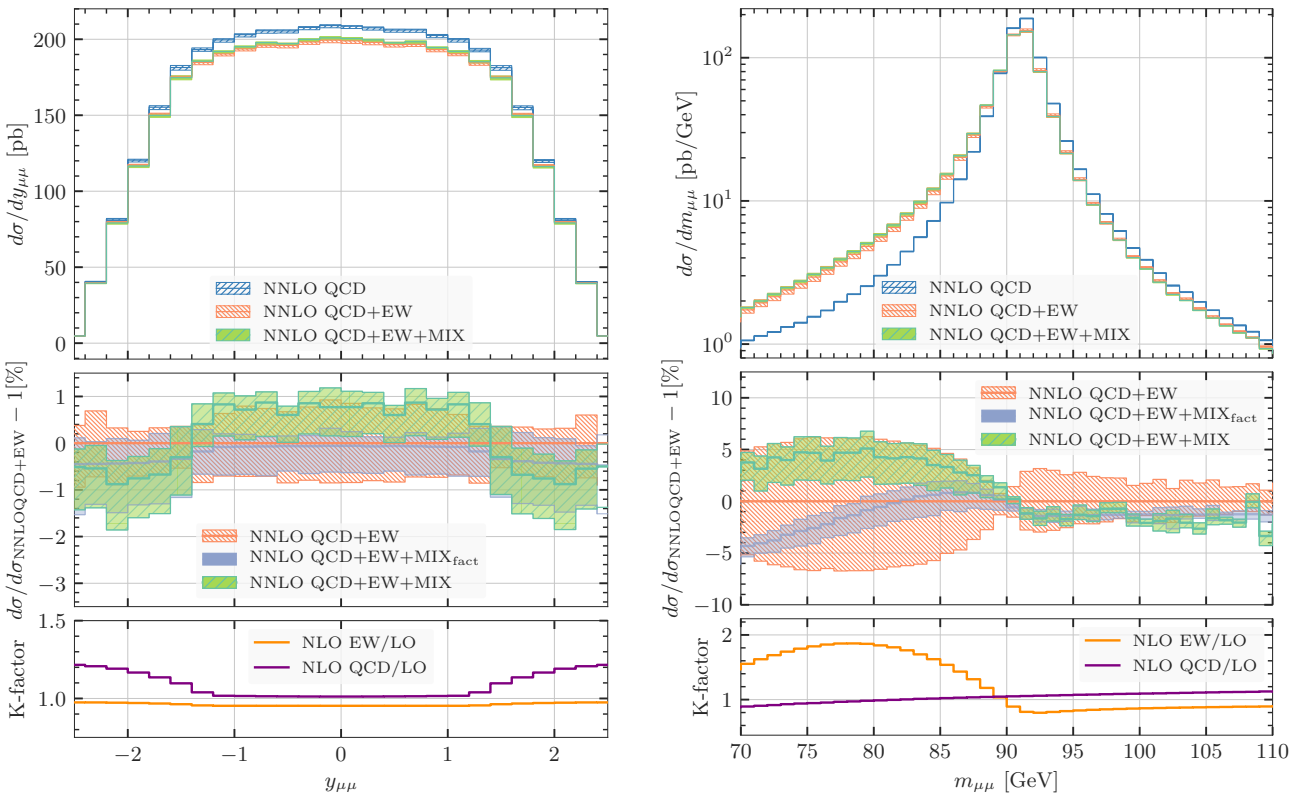

Figure 1: Predictions for the rapidity distribution (left) and the invariant mass distribution (right) of the final-state muon pair system. NLO EW and mixed QCD-EW corrections are additively included on top of the NNLO QCD prediction. The relative correction with respect to the additive combination NNLO QCD + (NLO) EW is showed in the middle panel, and the exact mixed correction is compared to the approximate factorised ansatz defined in the text. NLO-EW and NLO-QCD K-factor are displayed in the bottom panel.

the breakdown of the approximation in modelling the kinematical correlations occurring in the full real emission phase space. Furthermore, we notice that the inclusion of the mixed correction leads to a nice reduction of the uncertainty band. LB

(possibly, add other figs/comments.)

3 Results at high invariant masses

We consider the setup of Ref. [1], which defines the fiducial volume by requiring

$$m_{\ell\ell} > 200\,\text{GeV}, \quad p_{T,\ell^\pm} > 30\,\text{GeV}, \quad \sqrt{p_{T,\ell^+} p_{T,\ell^-}} > 35\,\text{GeV}, \quad |y_{\ell^\pm}| < 2.5\,. \tag{2}$$

We notice that in the calculation of Ref. [1] the leptons are treated as massless fermions. It is well known that fiducial cuts applied to the final-state massless, or "bare", leptons are, in general, not collinear safe with respect to the emission of a collinear photon off a final-state lepton. The definition of physical observables requires, then, the introduction of a recombination procedure of photons to a close-by lepton. This prevented the authors of Ref. [1] to directly

compare their calculation, valid for the dressed or calo leptons, to our results obtained for the case of bare massive muons.

Conversely, our framework, which retains the dependence on the mass of the final-state leptons, allows us to perform calculations for both bare and dressed leptons. This can be easily understood if we take seriously the fact that the mass of the lepton acts as the regulator of the final-state collinear singularity associated to the emission of a photon off a lepton. Indeed, the resulting dead-cone effect leads to a smooth suppression of the collinear photon radiation at the parton level. In combination with the cut on the transverse momentum of the dilepton system, again considered at the parton/bare level, this makes the real emission cross section finite. We can then apply the recombination procedure to each of the parton level event passing the r_{cut} requirement. This is perfectly analogous to what happens for jet cross sections computed with a local subtraction method. In passing by, we stress that the mass of the lepton must not be naively considered as an effective second cut-off parameter in our formalism. Our subtraction formula, indeed, retains the exact dependence on the mass of the lepton, thus not introducing any other approximation.

In other words, for bare leptons, the presence of infrared fiducial cuts, as the cut on the invariant mass of the dilepton system, spoils the KLN mechanism [2, 3] for infrared singularities. In the case the leptons are massive, the miscancellation of collinear singularities is made finite and exposed in leftover contributions logarithmically enhanced in the lepton mass. The photon-lepton recombination restores the cancellation of the infrared singularities between real and virtual contributions. The large logs in the mass of the lepton drop out the calculation and the radiative corrections become universal in the limit of a vanishing lepton mass. *(add references)* **LB**

This argument, which is valid at NLO EW, can be extended to the case of the mixed corrections. To summarise, we can retrieve the results of ref. [1] for dressed leptons within our framework by

1. applying the photon-lepton recombination to the real events passing the r_{cut} requirement at the parton level;

2. repeating the calculation for decreasing lepton masses and taking the limit of a vanishing mass.

We stress that the cut on the transverse momentum must be computed at the parton level event, before any recombination takes place. In practice, we can perform the calculation at a sufficiently small value of the lepton mass which can be even larger than the physical mass of the considered leptons, as long as power corrections terms can be safely neglected. For the sake of comparison, we reproduce the results for dressed electrons of Ref. [1] using as reference lepton mass the muon mass, $m_\ell = m_\mu = 105.658369\,\text{MeV}$. Results for a simplified splitting of partonic channels based on the presence or not of photons in the initial state are shown in Tab 3. In the top table, we report the comparison for dressed leptons. In the bottom one, we show results for the bare muons. At NLO, we performed the calculation with two independent subtraction schemes, qT subtraction and the local Catani-Seymour subtraction with massive dipoles [].

σ [fb]	$\sigma^{(0,0)}$	$\sigma^{(1,0)}$	$\sigma^{(0,1)}$	$\sigma^{(2,0)}$	$\sigma^{(1,1)}$
$q\bar{q}+qg+gg$ [1]	1561.42	340.37	-49.907	13.874	-15.77
$q\bar{q}+qg+gg$	1561.52(5)	340.34(7)	$-49.79(1)_{\rm CS}/-49.8(1)_{\rm QT}$	13(1)	$-15.1(6)_{\rm us}$ / $-16(1)_{\rm fid}$
$\gamma\gamma+q\gamma+g\gamma$ [1]	59.645	$--$	2.861	$--$	0.0598
$\gamma\gamma+q\gamma+g\gamma$	59.645(6)	$--$	$1.493(8)_{\rm CS}/1.5(5)_{\rm QT}$	$--$	0(4)

σ [fb]	$\sigma^{(0,0)}$	$\sigma^{(1,0)}$	$\sigma^{(0,1)}$	$\sigma^{(2,0)}$	$\sigma^{(1,1)}$
$q\bar{q}+qg+gg$	1561.52(5)	340.34(7)	$-96.07(2)_{\rm CS}/-96.1(2)_{\rm QT}$	13(1)	$-28(2)_{\rm us}$ / $-16(1)_{\rm fid}$
$\gamma\gamma+q\gamma+g\gamma$	59.645(6)	$--$	$-0.15(1)_{\rm CS}/-0.18(4)_{\rm QT}$	$--$	0(4)

Table 3: Comparison with the results obtained in Ref [] with a simplified channel splitting: photon induced and non-photon induced. At NLO, "CS" stands for Catani-Seymour subtraction and "q_T" for q_T subtraction. For the mixed corrections, the label "us" and "fid" refer to the way the fiducial cuts are applied, respectevely using user defined cuts or via the interfaced offered by MATRIX. In the latter case, this may lead to a further optimisation in the samplig of the phase space.

This is a first non-trivial test of our methodology. Indeed, the massive dipoles are designed in such a way to capture also the quasi-collinear singularity in the limit of a vanishing mass. In general, this leads to better numerical performances as the logarithms of the mass, which originally arise from the integration of the real contribution, are now supplied analytically by the integrated counterterm. Thus the combination with similar logs coming from the virtuals is numerical more stable and, at the same time, the real integration is alleviated as the integrand function becomes smoother.

A similar mechanism is not present in the q_T subtraction formalism, which, in addition, is plagued by sizeable linear power correction for the case of NLO EW corrections []. Despite this facts, we see from the comparison with the dipole calculation in Tab. [] that we can achieve a very good control of the NLO EW corrections, at the few per mille level. In addition, the results for the non-photon induced channel show a very good agreement with the one of Ref []. The difference between the dipole result and the one of Ref[] for the NLO EW corrections might be related to the fact we are using a finite lepton mass. Such a difference is well below the permyriad level, confirming that the power corrections in the lepton mass are indeed negligible for the choosen value. We find a discrepancy, instead, for the NLO EW corrections to photon induced channels between our two predictions, which are consistent among each others, and the reference result.

Turning to higher orders, we observe a nice agreement for the NNLO QCD correction. The choice of product cuts alleviates the problem of linear power correction in the q_T subtraction formalism, leading to a better convergence of the method. The situation is instead different for the mixed QCD-EW correction. In Tab. 4, we consider a more detailed breakdown into partonic channels. We observe a rather good agreement for the NNLO QCD in all individual channels. Turning to the mixed correction, we get a good agreement for the all-quark channel, which contains the genuine two-loop virtual contribution, and for the gluon-photon channel, while there is descrepancy of about 10% for the quark-photon one and a factor of 2 for the

σ [pb]	$\sigma_{\rm LO}$	$\sigma^{(1,0)}$	$\sigma^{(0,1)}$	$\sigma^{(2,0)}$	$\sigma^{(1,1)}$
$q\bar{q}$	1561.52(5)	340.3(3)	−49.77(5)	44.6(4)	−16.7(4)
qg	—	−0.6(2)	—	−32.7(2)	2.09(9)
$q\gamma$	—	—	−0.30(2)	—	−0.229(8)
$g\gamma$	—	—	—	–	0.2648(17)
gg	—	—	—	2.02(6)	—
$\gamma\gamma$	59.645(6)	—	1.798(7)	—	—

Table 4: The different perturbative contributions to the fiducial cross section (see Eq. (**??**)). The breakdown into the various partonic channels is also shown (see text).

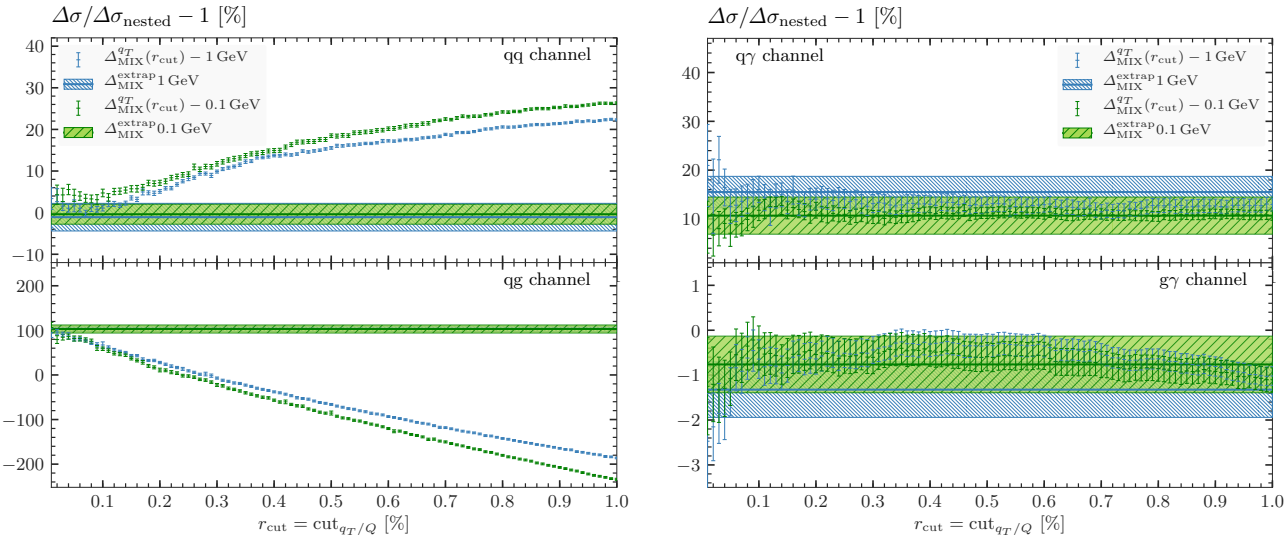

Figure 2: .

quark-gluon channel. To shed light on the discrepancy, in Fig. 2, we study the dependence on the cut-off parameter $r_{\rm cut}$ for the nominal lepton mass $m_\ell = m_\mu$ and for another mass value, $m_\ell = 1\,{\rm GeV}$. We observe that, within the statistical and extrapolation errors, the two runs nicely agrees providing a numerical confirmation that the residual dependence on the lepton mass, after the cancellation of large logarithms between real and virtual contributions, is power suppressed. Furthermore, this exercise strongly indicates that the cancellation of all IR divergencies underlying in our method do take place correctly, giving a reassuring check of the calculation.

Acknowledgements

References

[1] F. Buccioni, F. Caola, H. A. Chawdhry, F. Devoto, M. Heller, A. von Manteuffel, K. Melnikov, R. Röntsch, and C. Signorile-Signorile, *Mixed QCD-electroweak corrections to dilepton production at the LHC in the high invariant mass region*, arXiv:2203.11237.

[2] T. Kinoshita, *Mass singularities of Feynman amplitudes*, J. Math. Phys. **3** (1962) 650–677.

[3] T. D. Lee and M. Nauenberg, *Degenerate Systems and Mass Singularities*, Phys. Rev. **133** (1964) B1549–B1562. [,25(1964)].